American Mineralogist, Volume 89, pages 867–872, 2004

Aluminian low-Ca pyroxene in a Ca-Al-rich chondrule from the Semarkona meteorite

ALAN E. RUBIN*

Institute of Geophysics and Planetary Physics, University of California, Los Angeles, California, 90095-1567, U.S.A.

ABSTRACT

A Ca-Al-rich chondrule (labeled G7) from the Semarkona LL3.0 ordinary chondrite (OC) consists of 73 vol% glassy mesostasis, 22 vol% skeletal forsterite, 3 vol% fassaite (i.e., Al-Ti diopside), and 2 vol% Al-rich, low-Ca pyroxene. The latter phase, which contains up to 16.3 wt% Al_2O_3, is among the most Al-rich, low-Ca pyroxene grains ever reported. It is inferred that 20% of the tetrahedral sites and 13% of the octahedral sites in this grain are occupied by Al. Approximately parallel optical extinction implies that the Al-rich, low-Ca pyroxene grains are probably orthorhombic, consistent with literature data that show that Al_2O_3 stabilizes the orthoenstatite structure relative to protoenstatite at low pressure. The order of crystallization in the chondrule was forsterite, Al-rich low-Ca pyroxene, and fassaite; the residual liquid vitrified during chondrule quenching. Phase relationships indicate that, for a G7-composition liquid at equilibrium, spinel and anorthite should crystallize early and orthopyroxene should not crystallize at all. The presence of Al-rich orthopyroxene in G7 is due mainly to the kinetic failure of anorthite to crystallize; this failure was caused by quenching of the G7 precursor droplet. Aluminum preferentially enters the relatively large B tetrahedra of orthopyroxene; because only one tetrahedral size occurs in fassaite, this phase contains higher mean concentrations of Al_2O_3 than the Al-rich orthopyroxene (17.8 and 14.7 wt%, respectively). Chondrule G7 may have formed by remelting an amoeboid olivine inclusion that entered the OC region of the solar nebula during an episode of chondrule formation.

INTRODUCTION

Although most natural Mg-Fe low-Ca pyroxenes contain little Al (typically <3 wt%; Deer et al. 1978), high-pressure synthesis (18–27 kb or 1.8–2.7 GPa) of orthopyroxene from basaltic-composition melts under wet conditions can produce grains with substantial Al_2O_3 (3.6–8.8 wt%; Bultitude and Green 1967). This is consistent with the high-pressure origin inferred for most natural Al-rich, low-Ca pyroxene grains: e.g., 13.91 wt% Al_2O_3 in a ferrohypersthene from a hypersthene-cordierite-biotite granulite (Devaraju and Sadashivaiah 1971), and 7.72 wt% Al_2O_3 in a bronzite from a high-pressure megacryst in an alkaline lava (Binns et al. 1970).

There is one class of Al-rich orthopyroxenes that formed at low pressure. These occur in refractory inclusions and Ca-Al-rich chondrules in chondritic meteorites. We report here some Al-rich, low-Ca pyroxene grains that contain up to 16.3 wt% Al_2O_3. Grains of this phase occur in a chondrule in the Semarkona LL3.0 ordinary chondrite (OC), the least-metamorphosed OC known (e.g., Grossman 1985; Grossman and Rubin 1999). Semarkona fell in India in 1940 (Grady 2000); it has not been significantly affected by terrestrial weathering.

ANALYTICAL PROCEDURES

A previously prepared, 1.7 m wide back-scattered electron (BSE) mosaic image of Semarkona thin section USNM 1805-3 with a superimposed grid was used to label and locate chondrules of interest. Chondrule G7 contains the Al-rich, low-Ca pyroxene grains. BSE images of chondrule G7 were made with the LEO 1430VP scanning electron microscope (SEM) at UCLA using a 15 keV acceleration and a working distance of ~19 mm. I also examined the thin section microscopically in transmitted light and estimated the modal abundances of the chondrule constituents. Grain sizes were measured microscopically using a calibrated reticule. Mineral and mesostasis compositions were determined with the JEOL JXA-8200 electron microprobe at UCLA, using natural and synthetic standards, an accelerating voltage of 15 keV, a 15 nA sample current, 20 s counting times, and ZAF corrections.

RESULTS

Petrography of chondrule G7

Chondrule G7 is approximately circular in thin section with an apparent diameter of 540 μm (Fig. 1). This is close to the mean apparent diameter of chondrules in LL3 chondrites (570 μm; Nelson and Rubin 2002). The chondrule consists of 73 vol% light-brown glassy mesostasis, 22 vol% skeletal forsterite grains, 3 vol% fassaite grains (i.e., Al-Ti diopside), and 2 vol% Al-rich low-Ca pyroxene grains. Opaque phases are absent from the chondrule.

The forsterite grains range in size from 9×17 to 30×390 μm. Nearly every grain exhibits the chain structure described by Donaldson (1976) and comprises linked H-shaped units; many grains have small appendages (which Donaldson called "tongues") that connect adjacent units (Figs. 1 and 2). In some cases, generally aligned sets of two to five linked units are somewhat offset from each other. Some of the skeletal forsterite grains have prismatic terminations and appear subhedral. The forsterite grains are randomly oriented in the chondrule. One grain impinges upon the edge of a fassaite rim that surrounds the largest grain of Al-rich, low-Ca pyroxene (Figs. 2 and 3).

Fassaite occurs as 4–18 μm thick rims around all of the Al-

* E-mail: aerubin@ucla.edu

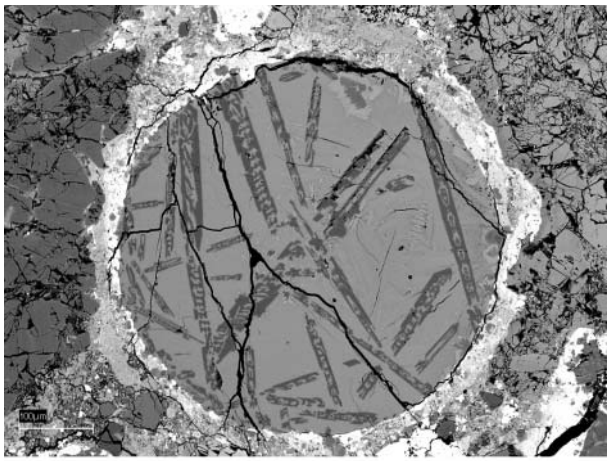

FIGURE 1. Ca-Al-rich chondrule G7 from the Semarkona LL3.0 ordinary chondrite. This chondrule consists mainly of elongated skeletal forsterite grains exhibiting a chain structure with H-shaped units (dark gray) and glassy mesostasis (medium gray). At the top and along the right side of the chondrule are a few small grains of Al-rich, low-Ca pyroxene (dark gray) surrounded by fassaite rims (light gray). The branching black lines that transect the chondrule are cracks. Back-scattered electron image. Scale bar at lower left is 100 μm in length.

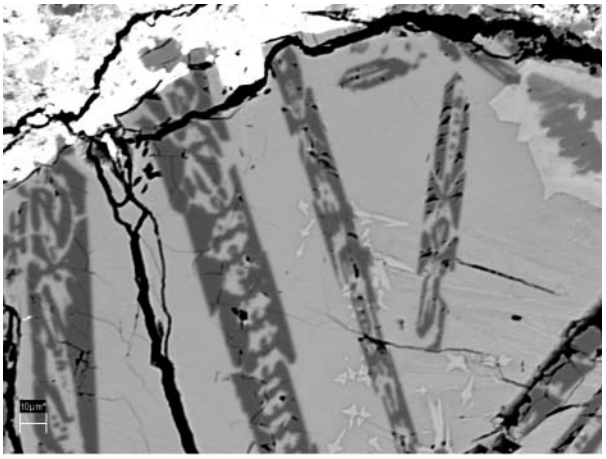

FIGURE 2. High-magnification view of forsterite grains (dark gray) in chondrule G7 showing the displacement of the stacked chains. Fassaite (light gray) has nucleated on some of the elongated forsterite grains. The largest grain of Al-rich, low-Ca pyroxene (dark gray) occurs at the upper right; the grain is surrounded by fassaite. A small elongated forsterite grain impinges upon the fassaite rim. Back-scattered electron image. Scale bar at lower left is 10 μm in length.

rich, low-Ca pyroxene grains (Fig. 3). It also occurs as individual 3–80 μm size euhedral, subhedral, and feathery crystals in the mesostasis and as 4–5 μm size crystals growing into the mesostasis from a forsterite substrate (Fig. 2). Most of the fassaite grains have angular margins (i.e., crystal faces) at the interface with mesostasis (Fig. 3).

The Al-rich, low-Ca pyroxene grains all occur near or along the edge of one side of the chondrule (Fig. 1). Some grains are blocky; others have a somewhat scalloped outline. The grains

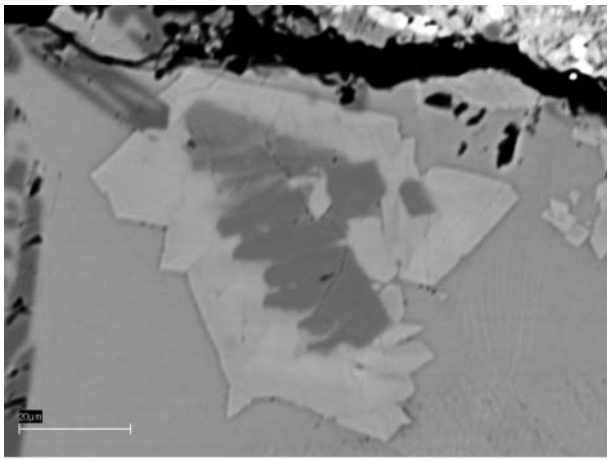

FIGURE 3. The largest grain of Al-rich low-Ca pyroxene (dark gray) surrounded by a fassaite rim (light gray) that exhibits angular faces at the interface with the glassy mesostasis (medium gray). A small skeletal forsterite grain (dark gray) at upper left impinges the fassaite. Back-scattered electron image.

TABLE 1. Mean compositions (wt%) of phases in chondrule G7

	Forsterite	Fassaite	Al-rich low-Ca pyx	Mesostasis
no. of grains	6	12	23	6
SiO_2	41.9	43.1	48.8	44.9
TiO_2	0.37	3.8	2.3	2.2
Al_2O_3	0.41	17.8	14.7	28.1
Cr_2O_3	0.04	0.20	0.13	0.08
FeO	0.14	0.18	0.13	0.12
MnO	0.03	0.06	0.03	0.05
MgO	56.1	13.7	31.2	5.6
CaO	0.28	20.9	2.4	17.4
Na_2O	<0.03	0.04	<0.03	0.26
K_2O	<0.03	<0.03	<0.03	<0.03
total	99.3	99.8	99.7	98.7
End-member	Fa 0.14	Fs 0.35	Fs 0.22	
		Wo 52.1	Wo 5.2	

range in size from 7 × 9 to 31 × 54 μm. All of them are surrounded by rims of fassaite (Fig. 3). Microscopic examination of the largest Al-rich, low-Ca pyroxene grain shows it to have approximately parallel optical extinction, consistent (but not conclusively so) with the phase being orthorhombic.

Mineral and mesostasis compositions

The mean compositions of forsterite, fassaite, Al-rich, low-Ca pyroxene, and mesostasis are listed in Table 1. All of the phases contain substantial concentrations of Al_2O_3.

The Al_2O_3 concentration in forsterite (0.41 wt%) exceeds that in normal low-FeO (type-IA) chondrules in Semarkona (0.03–0.35 wt%; Table 1 of Jones and Scott 1989). Other compositional differences between forsterite in chondrule G7 and type-IA chondrules include the appreciably lower FeO in G7 (0.14 vs. 0.45–2.41 wt%), lower Cr_2O_3 (0.04 vs. 0.06–1.11 wt%) and substantially higher TiO_2 (0.37 vs. 0.02–0.07 wt%). On the other hand, the forsterite CaO content (0.28 wt%) in G7 is close to the mean olivine CaO content of type-IA chondrules (0.31 wt%; Table 1 of Jones and Scott 1989).

Fassaite does not occur in typical type-IA chondrules. Nev-

TABLE 2. Compositions (wt%) and chemical formulae of selected analyses of Al-rich low-Ca pyroxene in chondrule G7 and in other refractory and moderately refractory objects from meteorites

	1	2	3	4	5	6
SiO_2	49.5	48.3	47.2	53.4	51.3	48.6
TiO_2	2.4	2.3	3.7	1.55	0.40	4.5
Al_2O_3	13.4	15.6	16.3	7.5	12.0	12.6
Cr_2O_3	0.14	0.18	0.14	0.71	0.27	0.88
FeO	0.09	0.11	0.20	0.35	0.52	1.1
MnO	0.04	<0.03	0.04	n.d.	n.d.	0.17
MgO	31.6	31.1	29.8	35.0	32.8	31.6
CaO	2.8	2.6	2.5	1.04	2.0	0.51
Na_2O	<0.03	<0.03	<0.03	n.d.	n.d.	<0.06
K_2O	<0.03	<0.03	<0.03	n.d.	n.d.	<0.04
Total	100.0	100.2	99.9	99.6	99.3	100.0
Numbers of ions on the basis of six O						
Si	1.68	1.64	1.61	1.81	1.75	1.66
Al^{IV}	0.32	0.36	0.39	0.17	0.24	0.32
Cr	0.00	0.00	0.00	0.02	0.01	0.02
Al^{VI}	0.21	0.26	0.26	0.13	0.24	0.19
Ti	0.06	0.06	0.10	0.04	0.01	0.12
Mg	1.60	1.57	1.51	1.77	1.66	1.60
Ca	0.10	0.10	0.09	0.04	0.07	0.02
Fe	0.00	0.00	0.00	0.01	0.02	0.03

Notes: n.d. = not determined. 1, 2, and 3 from chondrule G7; 4 from a refractory inclusion in the Allende CV3 carbonaceous chondrite (Fuchs 1969); 5 from an Al-diopside-rich chondrule in the Hammadah al Hamra 237 fine-grained Bencubbin-like meteorite (Krot et al. 2001); 6 from a plagioclase-rich chondrule in the Leoville CV3 carbonaceous chondrite (Krot et al. 2002).

TABLE 3. Compositions (wt%) of selected terrestrial occurrences of Al-rich low-Ca pyroxene

Source	1	2	3	4	5	6	7
SiO_2	49.32	48.48	52.35	46.91	53.16	47.30	48.85
TiO_2	0.81	0.52	0.23	0.51	1.35	0.63	0.24
Al_2O_3	6.39	7.21	7.72	8.26	10.55	10.81	13.91
Cr_2O_3	n.d.	n.d.	0.37	n.d.	n.d.	n.d.	n.d.
FeO	16.40	20.62	7.23	19.88	17.10	9.20	18.22
MnO	0.26	0.49	0.15	0.20	0.00	0.03	0.86
MgO	23.52	19.97	29.00	20.02	11.95	23.60	11.51
CaO	2.02	0.46	1.92	0.34	0.00	0.28	0.42
Na_2O	0.00	0.02	0.18	0.10	n.d.	n.d.	n.d.
K_2O	0.00	0.00	0.00	0.06	n.d.	n.d.	n.d.
Total	100.22	99.81	99.92	99.63	100.41	99.65	98.78

Notes: n.d. = not determined. 1 = Hypersthene from hypersthene peridotite from Finland. The analysis also includes 1.02 wt% Fe_2O_3, 0.03 wt% F and 0.45 wt% H_2O (Lokka 1943). 2 = Hypersthene from hypersthene-spinel-plagioclase hornfels from Scotland. The analysis also includes 1.97 wt% Fe_2O_3 and 0.07 wt% H_2O (Howie 1964). 3 = Orthopyroxene in high-pressure megacryst WA1 from alkaline lava from New South Wales. The analysis also includes 0.66 wt% Fe_2O_3 and 0.11 wt% NiO (Binns et al. 1970). 4 = Hypersthene from plagioclase-hypersthene-garnet granulite from Lapland. The analysis also includes 3.02 wt% Fe_2O_3 and 0.33 wt% H_2O (Eskola 1952). 5 = Hypersthene from charnockite from India. The analysis also includes 4.30 wt% Fe_2O_3 and 2.00 wt% H_2O (Rajagopalan 1946). 6 = Bronzite from pyrope-sapphirine rock from the Anabar Massif in northern Siberia. This analysis also includes 7.80 wt% Fe_2O_3 (Lutts and Kopaneva 1968). 7 = Ferrohypersthene from hypersthene-cordierite-biotite granulite from India. This analysis also includes 4.77 wt% Fe_2O_3 (Devarahu and Sadashivaiah 1971).

TABLE 4. Bulk composition (wt%) of chondrule G7, Ca-Al-rich chondrules and fragments from ordinary chondrites, and a hypothetical mixture of refractory minerals

	Bulk comp of G7	Normalized bulk comp of G7	Ca-Al-rich chondrules*	Ca-Al-rich fragments*	Refractory mixture†
SiO_2	44.2	44.7	49.1 (39.5–57.0)	41.4 (15.1–56.6)	44.6
TiO_2	1.8	1.8	0.67 (0.18–2.32)	0.73 (0.36–1.38)	–
Al_2O_3	20.5	20.8	16.1 (10.3–28.2)	21.0 (6.3–52.6)	20.9
Cr_2O_3	0.08	0.08	0.37 (0.07–1.39)	0.64 (0.16–3.2)	–
FeO	0.12	0.12	5.2 (0.43–14.5)	8.0 (2.15–19.3)	–
MnO	0.04	0.04	0.15 (0.02–0.39)	0.25 (0.05–0.98)	–
MgO	19.0	19.2	16.1 (3.8–33.8)	15.9 (7.0–28.7)	19.3
CaO	12.9	13.1	10.1 (4.3–19.6)	9.4 (3.1–14.7)	15.2
Na_2O	0.18	0.18	2.15 (0.04–4.7)	1.98 (0.05–4.7)	–
K_2O	<0.03	<0.03	0.11 (0.02–0.36)	0.20 (0.02–0.92)	–
Total	98.8	100.0	100.05	99.50	100.0

* Mean composition and range from Bischoff and Keil (1984).
† Calculation of bulk composition of a mixture consisting of the following pure end-member phases (in wt%): 55% anorthite, 28% forsterite, 16% diopside, and 1% spinel.

ertheless, the fassaite in G7 is within the range of fassaite compositions reported in refractory inclusions in CV carbonaceous chondrites (Table A3.16 of Brearley and Jones 1998). In particular, some fassaite grains in type-B inclusions in CV3 Allende are rather close in composition to fassaite in chondrule G7. One unusual feature of G7 fassaite is its relatively high Cr_2O_3 content (0.20 wt%); this value is higher than those in most refractory-inclusion fassaite grains (which generally contain <0.08 wt% Cr_2O_3).

Selected analyses of some Al-rich, low-Ca pyroxene grains in chondrule G7 are listed in Table 2. The Al_2O_3 contents range up to 16.3 wt%, far higher than that in the Al-rich orthopyroxene described by Fuchs (1969) from a refractory inclusion in the Allende CV3 carbonaceous chondrite (7.5 wt%; Table 2). The G7 low-Ca pyroxene grains have less FeO and Cr_2O_3 and more TiO_2 and CaO than the grains in the Allende inclusion. The G7 grains are also more aluminian than previously described low-Ca pyroxene grains from an Al-diopside chondrule in the Hammadah al Hamra 237 (HH237) fine-grained Bencubbin-like meteorite (12.0 wt%; Krot et al. 2001) or from a plagioclase-rich chondrule from the Leoville CV3 chondrite (12.6 wt%; Krot et al. 2002).

Analysis 3 of the G7 low-Ca pyroxene grains indicates that 20% of the tetrahedral sites and 13% of the octahedral sites are occupied by Al. These exceed the corresponding values for the other grains: 8.5 and 6.5% in Allende, 12 and 12% in HH237, and 16 and 10% in Leoville.

Terrestrial occurrences of Al-rich, low-Ca pyroxene all contain appreciable FeO (7–20 wt%) and Fe_2O_3 (1–8 wt%) (Table 3). The terrestrial grain with the most Al_2O_3 (13.91 wt% in a ferrohypersthene from a hypersthene-cordierite-biotite granulite from India) still has a lower Al_2O_3 content than the mean value in the Al-rich low-Ca pyroxene grains in chondrule G7 (14.7 wt%; Table 1). The terrestrial occurrences also differ in having less TiO_2 (0.23–1.35 wt%) than the G7 grains (2.0–3.7 wt%).

The G7 mesostasis averages 28.1 wt% Al_2O_3 and 17.4 wt% CaO (Table 1). These concentrations are similar to those of some glassy mesostases in type-IA chondrules in Semarkona, e.g., chondrule C61 contains 27.4 wt% Al_2O_3 and 20.7 wt% CaO (Table 3 of Jones and Scott 1989). However, the G7 mesostasis has lower FeO (0.12 vs. 0.28–1.37 wt%), lower Cr_2O_3 (0.08 vs. 0.19–1.18 wt%), and higher TiO_2 (2.2 vs. 0.51–1.51 wt%) than the type-IA mesostases.

Bulk composition

The bulk composition of chondrule G7 (Table 4) was calculated from the modal abundances (converted into wt% using estimated densities of the constituent phases: forsterite = 3.22; mesostasis = 2.70; Al-rich, low-Ca pyroxene = 3.21; fassaite = 3.30 (values in g/cm^3) and the mean compositions of the phases (Table 1). Bischoff and Keil (1984) defined Ca-Al-rich chondrules as those containing ≥10 wt% Al_2O_3 and ≤5.0 wt% Na_2O. It is clear that G7 (with 20.8 wt% Al_2O_3, 13.1 wt% CaO, and 0.18 wt% Na_2O) fits this definition. Table 4 shows that the

bulk composition of chondrule G7 lies within the concentration ranges of most elements (expressed as oxides) in Ca-Al-rich chondrules and Ca-Al-rich fragments in OC. The only exception is FeO, which is lower in G7 (0.12 wt%) than in the other objects (0.43–19.3 wt%).

DISCUSSION

Petrographic comparison to Ca-Al-rich chondrules

Chondrule G7 fits within the bulk compositional ranges of Ca-Al-rich chondrules in OC (except for having lower FeO) (Table 4). It is also similar in texture and mineralogy to many of these objects. Bischoff and Keil (1984) described a variety of Ca-Al-rich chondrule that is similar to G7 in having a barred-olivine-like texture consisting of narrow olivine laths surrounded by Ca-Al-rich glassy mesostasis that constitutes 50–70 vol% of the chondrule. Many of the Ca-Al-rich chondrules in OC contain fassaite and low-Ca pyroxene. Although Bischoff and Keil (1983a, 1983b, 1984) did not report any Al-rich, low-Ca pyroxene, such grains occur in some Ca-Al-rich chondrules (e.g., Krot et al. 2001).

Crystallization sequence

The Ca-Al-rich bulk composition of chondrule G7 implies that it formed from a relatively refractory precursor. The circular shape and high glass content of the chondrule (Fig. 1) indicate that it formed from a complete or nearly complete melt that cooled quickly. Any voids that existed in its precursor dustball would have collapsed during melting. Opaque phases that may have been present initially would have formed dense immiscible droplets; they could have been lost from the spinning molten chondrule via centrifugal action.

As chondrule G7 cooled, the randomly oriented, skeletal chain olivine grains must have crystallized very rapidly from the melt. The impingement of one of the forsterite grains on a fassaite rim around an Al-rich low-Ca pyroxene grain (Fig. 3) indicates that forsterite crystallized before fassaite. This sequence is also indicated by the occurrence of small fassaite grains growing at the surface of some forsterite grains. Because fassaite forms rims on the Al-rich low-Ca pyroxene grains, it is clear that low-Ca pyroxene also crystallized before fassaite.

Superpositioning relationships cannot be used to determine whether or not forsterite crystallized before Al-rich, low-Ca pyroxene, but the much higher modal abundance of forsterite suggests that forsterite was the first phase to crystallize. The Al-rich, low-Ca pyroxene crystallized shortly thereafter. Fassaite later nucleated and grew on the forsterite and Al-rich, low-Ca pyroxene grains. Finally, the chondrule cooled below the glass transition temperature and the residual liquid vitrified.

The bulk composition of G7 matches a hypothetical mixture of 55 wt% anorthite, 28 wt% forsterite, 16 wt% diopside, and 1 wt% spinel fairly closely (Table 4). When these proportions are plotted on the equilibrium pseudo-ternary diagram of the system forsterite-diopside-anorthite (Fig. 9.3 of Morse 1980), the point is within the forsterite field (albeit only marginally). This location is consistent with the conclusion that forsterite was the first phase to crystallize.

In the anorthite-forsterite-wollastonite-silica system, we can use a projection from the forsterite component of forsterite-saturated compositions onto the enstatite-anorthite-wollastonite plane (Fig. 4 of Longhi 1987); the bulk composition of chondrule G7 plots close to the boundary separating the spinel+forsterite and anorthite+forsterite fields. This finding indicates that, in addition to forsterite, spinel, and anorthite should crystallize at equilibrium from a G7-composition liquid. However, orthopyroxene should not crystallize at equilibrium from such a liquid.

The occurrence of Al-rich orthopyroxene in chondrule G7 must be due mainly to the kinetic failure of anorthite to crystallize. This failure probably resulted from chondrule quenching and rapid crystal growth. [In this regard, quenching has been shown capable of suppressing pyroxene crystallization in experimental charges with bulk compositions within the pyroxene stability field (e.g., Planner 1979; Tsuchiyama et al. 1980).] Because Al_2O_3 was not partitioned into anorthite in chondrule G7, it was available for incorporation into pyroxene.

Crystallization of Al-rich low-Ca pyroxene

Ultimately, the high bulk Al_2O_3 in chondrule G7 (20.8 wt%; Table 4) is responsible for the substantial Al_2O_3 contents of all of the phases (Table 1). The Al-rich, low-Ca pyroxene would not have crystallized from a system with appreciably lower Al_2O_3. The approximately parallel extinction of the Al-rich, low-Ca pyroxene grains suggests that this phase is orthorhombic. This inference is consistent with the report of O'Hara and Schairer (1963) that showed that Al_2O_3 greatly stabilizes the orthoenstatite structure relative to protoenstatite in the diopside-pyrope system at low pressure (i.e., 1 atm or 10^5 Pa). These workers produced orthopyroxene grains with high Al_2O_3 (up to 6 wt%) mainly because of the high Al_2O_3/CaO ratio at the pyrope end of the join.

Orthopyroxene has two kinds of Si-O chains with different configurations. The more fully extended A chain has smaller tetrahedra than the more compressed B chain (Deer et al. 1978). It seems likely that Al preferentially enters the B tetrahedra (Takeda 1972). In fassaite, the Si-O chains are all equivalent and only one size of tetrahedral site is available. This feature leads to complete disordering of the Si-Al substitution. Because more tetrahedral sites that can readily accommodate Al are available in fassaite (e.g., Peacor 1967), fassaite should generally contain higher concentrations of Al_2O_3 than coexisting orthopyroxene (Takeda 1972). This difference is, in fact, the case for chondrule G7 where the mean Al_2O_3 concentrations in fassaite and low-Ca pyroxene are 17.8 and 14.7 wt%, respectively (Table 1).

Origin of chondrule G7

The similarity in bulk composition between chondrule G7 and the mixture of 55 wt% anorthite, 28 wt% forsterite, 16 wt% diopside, and 1 wt% spinel (Table 4) is consistent with the idea that the chondrule was formed by melting a precursor dustball that contained these phases in approximately these proportions. These are also the principal phases that constitute amoeboid olivine inclusions (AOI) in carbonaceous chondrites (e.g., Grossman and Steele 1976; McSween 1977a; Kornacki and Wood 1984; Hashimoto and Grossman 1987; Aléon et al. 2002; Chizmadia et al. 2002). In a comprehensive study of AOI in CO3.0 Y-81020, Itoh et al. (unpublished manuscript 2003) found that the proportions of forsterite, diopside, and anorthite vary appreciably; some

AOI have proportions of these phases that approximate those that match the bulk composition of chondrule G7. In addition, a few AOI contain up to 3 vol% spinel (Chizmadia et al. 2002; Komatsu et al. 2001, 2003). Accordingly, it is possible that chondrule G7 formed from an AOI precursor.

This scenario is speculative. Although OC contain rare refractory inclusions (e.g., MacPherson et al. 1988), AOI have not been reported. The apparent absence of AOI in OC is in contrast to the case for most carbonaceous-chondrite groups (i.e., CM, CO, CV, CR), whose members contain a few vol% of both AOI and refractory inclusions (e.g., McSween 1977a, 1977b, 1977c, 1979; Weisberg et al. 1993). It seems possible that AOI were mixed into the OC region of the solar nebula but were remelted during chondrule formation. Because most normal ferromagnesian chondrules appear to have experienced more than one melting episode (e.g., Rubin and Krot 1996; Wasson and Rubin 2003), it is plausible to infer that any AOI that might have been present in the OC chondrule-formation region also could have been remelted. A remelted AOI could resemble chondrule G7 in texture and bulk composition.

The O-isotopic composition of an AOI that was remelted in the OC-chondrule-formation region is difficult to predict. Spinel, diopside, anorthite, and forsterite in AOI in Y-81020 are all enriched in ^{16}O (with both $\delta^{17}O$ and $\delta^{18}O$ approximately equal to –40‰; Itoh et al. unpublished manuscript 2003). Ca-Al-rich chondrules in OC that formed from AOI would have inherited this O-isotopic composition from the precursor AOI unless they underwent isotopic exchange with ^{16}O-poor nebular gas in the OC-chondrule-formation region (Krot et al. 2002) during the time that they were molten.

The rare refractory inclusions in OC could have been late additions that largely post-dated chondrule formation. If so, they would have escaped remelting and retained their ^{16}O-rich compositions.

ACKNOWLEDGMENTS

I thank W.A. Dollase, J.T. Wasson, and A.N. Krot for helpful discussions and F.T. Kyte for technical assistance. Useful comments were provided by D.R. Peacor, H. Takeda, L. Grossman, and C.T. Prewitt. H. Haack kindly forwarded some literature to me. The paper benefited from reviews by J. Longhi and J. Jones. I am grateful to the Smithsonian Institution for the loan of Semarkona thin section USNM 1805-3. This work was supported by NASA grant NAG5-12967.

REFERENCES CITED

Aléon, J., Krot, A.N., and McKeegan, K.D. (2002) Calcium-aluminum-rich inclusions and amoeboid olivine aggregates from the CR carbonaceous chondrites. Meteoritics and Planetary Science, 37, 1729–1755.

Binns, R.A., Duggan, M.B., Wilkinson, J.F.G., and Kalocsai, G.I.Z. (1970) High pressure megacrysts in alkaline lavas from northeastern New South Wales. American Journal of Science, 269, 132–168.

Bischoff, A. and Keil, K. (1983a) Ca-Al-rich chondrules and inclusions in ordinary chondrites. Nature, 303, 588–592.

———(1983b) Catalog of Al-rich chondrules, inclusions and fragments in ordinary chondrites. University of New Mexico Institute of Meteoritics Special Publication, 22, 1–32.

———(1984) Al-rich objects in ordinary chondrites: Related origin of carbonaceous and ordinary chondrites and their constituents. Geochimica et Cosmochimica Acta, 48, 693–709.

Brearley, A.J. and Jones, R.H. (1998) Chondritic meteorites. In J.J. Papike, Ed., Planetary Materials, 36, pp. 313–398. Reviews in Mineralogy, Mineralogical Society of America, Washington, D.C.

Bultitude, R.J. and Green, D.H. (1967) Experimental study at high pressures on the origin of olivine nephelinite and olivine melilite nephelinite magmas. Earth and Planetary Science Letters, 3, 325–337.

Chizmadia, L.J., Rubin, A.E., and Wasson, J.T. (2002) Mineralogy and petrology of amoeboid olivine inclusions in CO3 chondrites: Relationship to parent-body aqueous alteration. Meteoritics and Planetary Science, 37, 1781–1796.

Deer, W.A., Howie, R.A., and Zussman, J. (1978) Rock-forming Minerals, Volume 2A—Single-chain Silicates, 668 p. Wiley, New York.

Devaraju, T.C. and Sadashivaiah, M.S. (1971) Some orthopyroxene-bearing rocks constituting an integral part of high-grade metapelites of Satnur-Halaguru area, Mysore State. Journal of the Geological Society of India, 12, 1–13.

Donaldson, C.H. (1976) An experimental investigation of olivine morphology. Contributions to Mineralogy and Petrology, 57, 187–213.

Eskola, P. (1952) On the granulites of Lapland. American Journal of Science, (Bowen Vol.), 133–172.

Fuchs, L.H. (1969) Occurrence of cordierite and aluminous orthoenstatite in the Allende meteorite. American Mineralogist, 54, 1645–1653.

Grady, M.M. (2000) Catalogue of Meteorites, 5th Ed., 689 pp. Cambridge, U.K.

Grossman, J.N. (1985) Semarkona: The least metamorphosed ordinary chondrite (abstract). Meteoritics, 20, 656–657.

Grossman, J.N. and Rubin, A.E. (1999) The metamorphic evolution of matrix and opaque minerals in CO chondrites (abstract). Lunar and Planetary Science, 30, 1639–1640.

Grossman, L. and Steele, I.M. (1976) Amoeboid olivine aggregates in the Allende meteorite. Geochimica et Cosmochimica Acta, 40, 149–155.

Hashimoto, A. and Grossman, L. (1987) Alteration of Al-rich inclusions inside amoeboid olivine aggregates in the Allende meteorite. Geochimica et Cosmochimica Acta, 51, 1685–1704.

Howie, R.A. (1964) Some orthopyroxenes from Scottish metamorphic rocks. Mineralogical Magazine, 33, 903–911.

Jones, R.H. and Scott, E.R.D. (1989) Petrology and thermal history of type IA chondrules in the Semarkona (LL3.0) chondrite. Proceedings of the Lunar and Planetary Science Conference, 19, 523–536.

Komatsu, M., Krot, A.N., Petaev, M.I., Ulyanov, A.A., Keil, K., and Miyamoto, M. (2001) Mineralogy and petrography of amoeboid olivine aggregates from the reduced CV3 chondrites Efremovka, Leoville and Vigarano: Products of nebular condensation, accretion and annealing. Meteoritics and Planetary Science, 36, 629–641.

Komatsu, M., Miyamoto, M., Krot, A.N., and Keil, K. (2003) EBSD study of amoeboid olivine aggregates in the Y-81020 CO3.0 chondrite (abstract). Meteoritics and Planetary Science, 38, A75.

Kornacki, A.S. and Wood, J.A. (1984) Petrography and classification of Ca,Al-rich and olivine-rich inclusions in the Allende CV3 chondrite. Proceedings of the Lunar and Planetary Science Conference, 14, B573–B587.

Krot, A.N., McKeegan, K.D., Russell, S.S., Meibom, A., Weisberg, M.K., Zipfel, J., Krot, T.V., Fagan, T.J., and Keil, K. (2001) Refractory calcium-aluminum-rich inclusions and aluminum-diopside-rich chondrules in the metal-rich chondrites Hammadah al Hamra 237 and Queen Alexandra Range 94411. Meteoritics and Planetary Science, 36, 1189–1216.

Krot, A.N., Hutcheon, I.D., and Keil, K. (2002) Plagioclase-rich chondrules in the reduced CV chondrites: Evidence for complex formation history and genetic links between calcium-aluminum-rich inclusions and ferromagnesian chondrules. Meteoritics and Planetary Science, 37, 155–182.

Lokka, L. (1943) Beitrage zur Kenntnis des Chemismus der finnischen Minerale. Bulletin de la Commission géologique de Finlande, 129, 1–72.

Longhi, J. (1987) Liquidus equilibria and solid solution in the system $CaAl_2Si_2O_8$-Mg_2SiO_4-$CaSiO_3$-SiO_2 at low pressure. American Journal of Science, 287, 265–331.

Lutts, B.G. and Kopaneva, L.H. (1968) A pyrope-sapphirine rock from the Anabar massif and its conditions of metamorphism. Doklady Academy of Sciences, U.S.S.R., Earth Science Section, 179, 161–163.

MacPherson, G.J., Wark, D.A., and Armstrong, J.T. (1988) Primitive material surviving in chondrites: Refractory inclusions. In J.F. Kerridge and M. S. Matthews, Eds., Meteorites and the Early Solar System, p. 746–807. University of Arizona Press, Tucson.

McSween, H.Y. (1977a) Chemical and petrographic constraints on the origin of chondrules and inclusions in carbonaceous chondrites. Geochimica et Cosmochimica Acta, 41, 1843–1860.

——— (1977b) Carbonaceous chondrites of the Ornans type: A metamorphic sequence. Geochimica et Cosmochimica Acta, 41, 477–491.

——— (1977c) Petrographic variations among carbonaceous chondrites of the Vigarano type. Geochimica et Cosmochimica Acta, 41, 1777–1790.

——— (1979) Alteration in CM carbonaceous chondrites inferred from modal and chemical variations in matrix. Geochimica et Cosmochimica Acta, 43, 1761–1770.

Morse, S.A. (1980) Basalts and Phase Diagrams: An Introduction to the Quantitative Use of Phase diagrams in Igneous Petrology, 493 pp. Springer, New York.

Nelson, V.E. and Rubin A. E. (2002) Size-frequency distributions of chondrules and chondrule fragments in LL3 chondrites: Implications for parent-body fragmentation of chondrules. Meteoritics and Planetary Science, 37, 1361–1376.

O'Hara, M.J. and Schairer J.F. (1963) The join diopside-pyrope at atmospheric pressure. Carnegie Institution of Washington Yearbook, 62, 107–115.

Peacor, D.R. (1967) Refinement of the crystal structure of a pyroxene of formula

$M_I M_{II} (Si_{1.5}Al_{0.5})O_6$. American Mineralogist, 52, 31–41.
Planner, H.N. (1979) Chondrule thermal history implied from olivine compositional data, Ph.D. thesis, University of New Mexico, Albuquerque.
Rajagopalan, C. (1946) Studies in charnockites from St. Thomas Mount, Madras—Part I. Proceedings of the Indian Academy of Science, 24, 315–331.
Rubin, A.E. and Krot, A.N. (1996) Multiple heating of chondrules. In R.H. Hewins, R.H. Jones, and E.R.D. Scott, Eds., Chondrules and the Protoplanetary Disk, p. 173–180. Cambridge, U.K.
Takeda, H. (1972) Crystallographic studies of coexisting aluminian orthopyroxene and augite of high-pressure origin. Journal of Geophysical Research, 77, 5798–5811.
Tsuchiyama, A., Nagahara, H., and Kushiro, I. (1980) Experimental reproduction of textures of chondrules. Earth and Planetary Science Letters, 48, 155–165.
Wasson, J.T. and Rubin, A.E. (2003) Ubiquitous low-FeO relict grains in type II chondrules and limited overgrowths on phenocrysts following the final melting event. Geochimica et Cosmochimica Acta, 67, 2239–2250.
Weisberg, M.K., Prinz, M., Clayton, R.N., and Mayeda, T.K. (1993) The CR (Renazzo-type) carbonaceous chondrite group and its implications. Geochimica et Cosmochimica Acta, 57, 1567–1586.

MANUSCRIPT RECEIVED AUGUST 13, 2003
MANUSCRIPT ACCEPTED JANUARY 27, 2004
MANUSCRIPT HANDLED BY LINDSAY KELLER